*fishes*

MDPI

*Article*

# Exploring Growth Patterns of *Maurolicus muelleri* across Three Northeast Atlantic Regions

**Paula Alvarez [1,*], Naroa Aldanondo [1], Alina M. Wieczorek [2], Thibault Cariou [3], Guillermo Boyra [1], Eduardo Grimaldo [4,5], Webjørn Melle [6] and Thor Klevjer [6,†]**

1 AZTI Marine Research, Basque Research and Technology Alliance (BRTA), Herrera kaia, Portualdea z/g, 20110 Pasaia, Gipuzkoa, Spain; naldanondo@azti.es (N.A.); gboyra@azti.es (G.B.)
2 National Institute of Water and Atmosphere Research (NIWA), 301 Evans Bay Parade, Wellington 6021, New Zealand; alinamadita.wieczorek@niwa.co.nz
3 Marine Institute (MI), Rinville, Oranmore Co Galway, H91 R673 Galway, Ireland; thibault.cariou@marine.ie
4 SINTEF Ocean, Brattørkaia 17C, 7010 Trondheim, Norway
5 Norwegian College of Fishery and Aquatic Science, UiT the Arctic University of Norway, Breivika, 9037 Tromsø, Norway
6 Institute of Marine Research (IMR), Nordnesgaten 50, 5005 Bergen, Norway; webjoern.melle@hi.no (W.M.)
* Correspondence: palvarez@azti.es
† Deceased author.

**Abstract:** *Maurolicus muelleri* is an important component of mesopelagic ecosystems; nevertheless, we possess only limited knowledge about its biological features. We collected samples of *M. muelleri* from six scientific surveys between 2019 and 2021 in three geographical areas in the Northeast Atlantic waters (from South to North): the Bay of Biscay, the Celtic Sea, and the Norwegian Sea. Geographical variations in otolith growth, fish age, length, weight, and condition, as well as length–weight relationships and von Bertalanffy growth models (VBGMs), were investigated. Length-weight relationships revealed differences associated with the fish's origin, paralleling the annual and daily otolith growth. VBGM parameters increased progressively northwards, in accordance with Bergmann's rules. Fish length was positively related to the otolith radio, and Lee's phenomenon was undetected. The impact of environmental variables, such as temperature and food availability, is debated, with these considered potential drivers of this variability. Populations may belong to separated units, either genetically or morphologically, representing differences in biological parameters as a signal of geographical divergence.

**Keywords:** *Maurolicus muelleri*; otoliths; Lee's phenomenon; von Bertalanffy growth model; fish condition

**Key Contribution:** This study examines the growth patterns of *M. muelleri* in the Northeastern Atlantic from a broad geographical perspective, providing new evidence of the biological diversity within this population. The impact of environmental variables, such as temperature and food availability, is discussed as potential drivers of this variability while considering the possibility of these populations belonging to separate biological units.

check for updates

**Citation:** Alvarez, P.; Aldanondo, N.; Wieczorek, A.M.; Cariou, T.; Boyra, G.; Grimaldo, E.; Melle, W.; Klevjer, T. Exploring Growth Patterns of *Maurolicus muelleri* across Three Northeast Atlantic Regions. *Fishes* **2024**, *9*, 250. https://doi.org/10.3390/fishes9070250

Academic Editor: Gioele Capillo

Received: 24 May 2024
Revised: 18 June 2024
Accepted: 20 June 2024
Published: 26 June 2024



## 1. Introduction

*Maurolicus muelleri* (Gmelin) is a common mesopelagic fish species widely distributed in the North Atlantic waters [1]. It can be found across numerous mesopelagic ecosystems. *M. muelleri* occupies areas close to continental slopes or may be associated with land masses, and it is usually found at a depth of about 50–400 m [2].

Studies on the biology of *M. muelleri* worldwide are not extensive compared to other epipelagic or benthic fish species. This is partially due to the limited accessibility of the areas they inhabit and partially due to the lack of commercial interest in these fish [3]. Areas with more information on the biology and distribution of *M. muelleri* are Norwegian

fjords, with many of those studies going back more than 30 years [4,5]. *M. muelleri* is a small (4–5 cm) and short-lived fish (with a maximum lifespan of 5 years). Only a small proportion of the population reaches the age of 3 years [4], and in other areas, such as the Rockall Trough, longevity may be as little as 1 year, although a few specimens of 2 years old have been found [6].

Fish age, along with other biological parameters, plays a significant role in reaching sustainable fishery resource management [7]. Therefore, determining the age of fish requires knowledge to understand the historical dynamics of fish populations and to predict future population trends, especially by estimating growth and mortality rates [8,9]. For *M. muelleri*, few studies have provided information regarding the age structure, longevity, and growth rates by analysing daily and annual increments in otoliths [4,5]. A unique attempt to validate the method of annual age determination was reported in the early eighties [4]. However, the effect of the relative otolith size and the occurrence of Lee's phenomenon in *M. muelleri* have rarely been investigated [10]. Lee's phenomenon refers to otoliths of slow-growing fish, which tend to be larger and heavier than those of fast-growing fish of the same size, whether on a daily or yearly scale [11], cited in [10]. If this occurs, the back-calculated lengths from old age groups may be underestimated.

Differences in environmental parameters such as temperature or food availability may be responsible for geographical variations in the species' life history characteristics. For species as widely distributed as *M. muelleri*, information on environmental parameters must be collected on a regional basis. Differences in growth rates between individuals inhabiting oceanic and fjord environments can be attributed to different temperatures and salinity regimes [5,12]. Mortality is also shaped by environmental patterns: [4,5] observed higher adult mortality rates in offshore populations, likely associated with lower food availability compared to fjords. They also described that variability in maximum size or age was observed at regional scales, likely due to differences in environmental conditions.

The geographic distribution of Maurolicus has been described well using phylogenetic analyses [1]. Globally, the authors differentiated four main groups with a clear geographic distribution. With regard to *M. muelleri*, its distribution is confined to the North Atlantic region, from the Barents Sea and Iceland to the Mediterranean Sea (formerly two species). In the Eastern Atlantic, the species is distributed along the coast of Europe, from Norway to the northwest coast of Africa. It is also found in the Western Atlantic and waters off the coast of North America, including Canada and the United States.

The main purpose of this study was to estimate age-based demographic parameters of *M. muelleri* in the NEA waters. Otolith growth and age were examined using data collected through surveys conducted in 2019 and 2021. The determined life history features were then compared among geographical regions and interpreted based on the environmental conditions that each region sustains.

## 2. Materials and Methods

### *2.1. The Study Area*

The study area, the Northeast Atlantic (NEA), encompasses an extensive region from 42° N to 63° N and 2° E to 25° W (Figure 1) with a wide variety of hydrographic conditions that reflect different geographical areas, which further vary with season. For instance, in the NEA, temperatures at 20 m depth can range from <8 °C to >20 °C, increasing gradually from north to south [13]. The NEA region undergoes a predominant seasonal cycle in primary production, where the peak intensifies and is delayed as latitudes increase [14], along with a shortened duration of blooms [15].

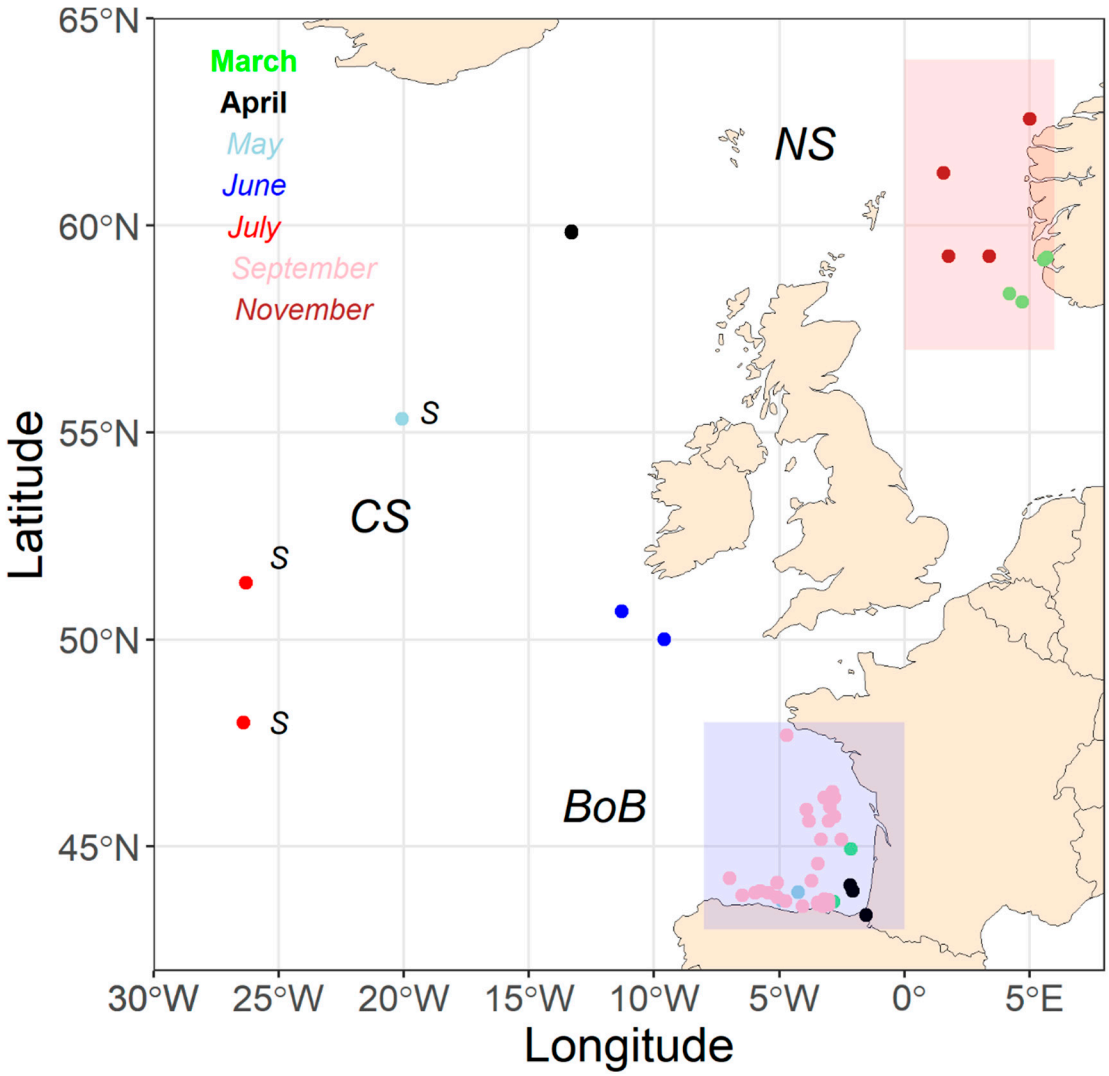


**Figure 1.** Spatial distribution of *M. muelleri* collected within the context of the MEESO project. Points marked with "s" were collected by SINTEF in 2016 and 2017. The Bay of Biscay (BoB) and the Norwegian Sea (NS) are encircled to separate them from the Celtic Sea (CS) region.

### *2.2. Sample Collection*

Pearlsides (*M. muelleri*) were collected in three distinct geographical areas, namely, the Bay of Biscay (BoB), comprising the area between 43° N and 48° N; the Celtic Sea (CS), which includes the samples collected between 50° N and 60° N; and the North Sea areas (NS), represented by the samples taken between 58° N and 62° N (Figure 1 and Table 1).

Before each campaign, a protocol outlining procedures for biological sampling was sent to the collaborators with a desirable number of individuals per haul.

Retained specimens were divided into three batches for preservation: one subsample was kept frozen, another was kept in 4% formaldehyde, and the third was kept in 90% ethanol. Recorded metadata for each haul included the position of capture, date and time, sampler and bottom depth, temperature, salinity, and, where available, dissolved oxygen.

In the Bay of Biscay, most of the data and samples were collected in September 2019 and 2020 during the JUVENA acoustic survey [16], and some additional samples were provided by the international mackerel and horse mackerel surveys (MEGS) in spring 2019 and BIOMAN in spring 2020 (Figure 1 and Table 1). Details on sampling methodologies can be found in [17], and details on fishing nets are listed in Table 2.

In the Celtic Seas, data and samples were collected during the International Blue Whiting Spawning Stock Survey (IBWSS) in April 2021 and during the Western European

Shelf Pelagic Acoustic Survey (WESPAS) in June 2020 and 2021 in the area of the Celtic Sea and West of Ireland (Figure 1 and Table 1) [18–20].

To extend the sampling periods and number of samples, an additional set of data collected by SINTEF 2016 and 2017 [21] in the Mid-Atlantic Ridges in spring and summer were included in the analysis, increasing the amount of data (Figure 1 and Table 1). The nets used to collect the biological samples are described in Table 2.

In the North Sea and the Norwegian Sea, samples were provided from two surveys specifically designed for the MEESO project: the first survey was an exploratory survey carried out North of the Rockall Bank and the Norwegian Sea in November 2019 aboard the MS *Birkenland* (Figure 1). The second survey was conducted by the Marine Institute (IMR, Bergen) during its spring survey in the North Sea and Norwegian fjords in March 2020. Table 2 shows the main characteristics of the fishing nets used during the campaigns.

**Table 1.** A summary of surveys that contributed biological samples. TS: sea surface temperature; T100m: the temperature at a 100 m depth. [1] Surveys outside of the MEESO project. These samples were used for the length-at-age model exclusively. [2] The temperatures at 10 and 50 m depths [22] and [3] the temperature at a fishing depth [21].

| Area | Survey | Period | TS (°C) | T100m (°C) | Nb. Individuals |
|---|---|---|---|---|---|
| BoB | MEGS | 1–6 Apr19 | 12.6 | 12.6 | 62 |
| | BIOMAN | 4–10 May20 | 12.7 | 12.7 | 138 |
| | JUVENA | 1–30 Sep19 | 20.01 | 17.4 | 874 |
| | JUVENA | 1–30 Sep20 | 21.13 | 17.6 | 500 |
| CS | WESPAS | 13-Jun20 | 14 | 9.9 | 152 |
| | IBWSS | 4-Apr21 | 8–11.5 | 8.9 | 94 |
| | WESPAS | 24-Jun21 | 13 | 11.1 | 149 |
| NS | MEESO-SINTEF | 7–19Nov19 | 10 | 7.5 [2] | 199 |
| | MEESO-IMR | 11–16 Mar20 | 6.2 | NA | 113 |
| CS [1] | SINTEF [1] | 4-Jul16 | 5.2 [3] | NA | 95 |
| | SINTEF [2] | 18–21May17 | 12.3 [3] | 14.8 [3] | 50 |

**Table 2.** A brief description of the fishing nets used to collect *M. muelleri* in the different campaigns.

| Survey | Type/Vessel | Region | Objective | Net Description |
|---|---|---|---|---|
| JUVENA<br>MEGS<br>BIOMAN | Opportunistic/R/V Ramom Margalef<br>R/V Emma Bardan | BoB | Anchovy juveniles<br>Mackerel/horse mackerel<br>Anchovy adults and sardine | Pelagic trawl, 12 × 25 m, mesh of 4–8 mm |
| WESPAS | Opportunistic/RV Celtic Explore | CS | Pelagic species | Pelagic midwater trawl (85 m length, fishing circle of 420 m, wing mesh size of 2.4 m graded through to codend of 10 cm) |
| IBWSS | Opportunistic/RV Celtic Explore | CS | Blue whiting | Pelagic trawl, 82 × 73 m, and Macroplankton trawl |
| SINTEF | "Ad hoc"<br>MS Birkeland | CS | Mesopelagic fish | 800 m circumference mesopelagic fish trawl, 10 mm innernet codend, 16 mm innernet extension piece, 20 mm innernet in the trawl belly. Small-meshed (10 mm) covers in the belly and extension piece |
| SINTEF | "Ad hoc"/MS Birkeland | NS | Mesopelagic fish | |
| IMR | "Ad hoc"/R/V Kristine Bonnevie | NS | Mesopelagic fish | Fine-meshed mesopelagic trawl, 8 mm mesh size |

### 2.3. Laboratory Procedures

The total length (TL), standard length (SL), total weight (TW) (Figure 2a), eviscerated weight (the weight of the fish excluding the gonads, digestive tract, liver, and heart), and gonad weight were measured for each individual, and the otoliths were extracted. Further information on laboratory procedures can be consulted in [18].

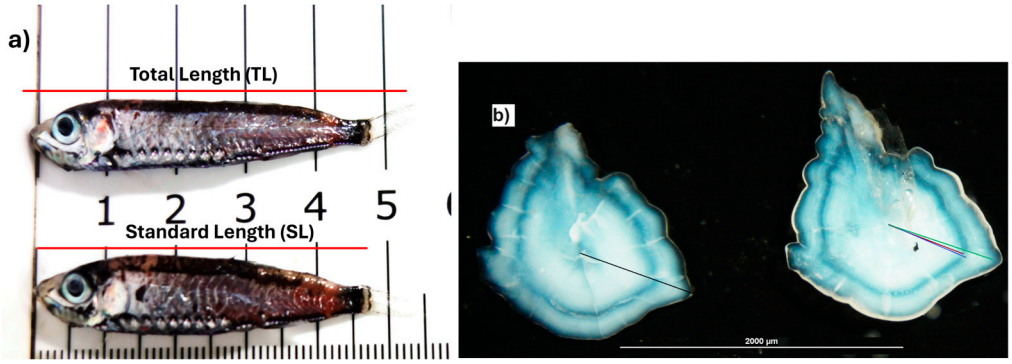


**Figure 2.** (**a**) An image showing two specimens of *M. muelleri* indicating the total length (TL) and the standard length (SL) measured. (**b**) An image showing a pair of sagittal otoliths of *M. muelleri* (age of 2) illustrating the radio (left otolith) and the radii of each annual increment measured (right otolith).

Otolith examination: Whole sagittal otoliths were immersed in fresh water and examined under a stereomicroscope at 20 × 25 magnification using reflected light and a black background. Their age was determined by examining annual increments, and calculations were made assuming a birth date of 1 January. The criteria for age assignation were the same as for anchovy [23]. More details of the procedure can be found in [17].

A subsample of 336 otoliths comprising individuals from the 3 regions and encompassing the respective sizes ranges per sex were selected to obtain various measurements. Measurements of maximum radio and the corresponding radii of each annual increment (from the core to the outer edge of the increment) (Figure 2) were obtained with an image analysis system.

For daily growth estimation, otoliths of 11 specimens captured in the Bay of Biscay were processed as described in [24]. Then, the otoliths (right sagitta) were analysed using a light microscope and an image analyser (Visilog, TNPC Software, v.5.02, Ifremer, France). The central part of otoliths was read at ×1000 magnification in immersion oil, and the outer part was analysed at ×200. Composite image files were constructed to enable the reader to scroll across the complete otolith image during analysis. All increments were counted, and the distance between increments was measured along the longest axis from the core to the edge of the otolith on the post-rostrum side. Increments were assumed to be daily from the first increment. Additionally, the hatch date was calculated by subtracting otolith increment counts from the day individuals were collected in the field.

### 2.4. Statistical Analysis

The TW–SL relationship was estimated for each region using a power equation via non-linear regression. Otolith radius (OR)-SL relationships were estimated for each region using linear models. The equality of the models was tested by conducting an ANCOVA analysis. This test evaluated the null hypothesis of the equality of regressions estimated by region with a significance level of 5% ($\alpha = 0.05$) [25]. Differences between the expected value from isometric growth and the values of the regression coefficient (b) were compared using a *t*-test [26]. This test evaluated the null hypothesis H0: b = 3 in TW-SL relationship and H0: b = 1 in OR-SL relationships, with a significance level of 5% ($\alpha = 0.05$) [25]. The equality of SL between regions within age classes was analysed using a two-way ANOVA.

The Le Cren [27] condition factor was estimated to quantify the individual state of health.

The Stomach Somatic Index (SSI), calculated as the stomach weight divided by the eviscerated weight, was estimated to quantify the feeding activity of fish.

Equality amongst regions was assessed using the Mann–Wilcox test, and a pairwise comparison of this parameter was performed using Dunn's multiple comparison test.

The von Bertalanffy growth model (VBGM) was selected to determine the growth in length (SL, mm) with age (years) of the individuals. The VBGMs were constructed by areas. Inbio 2.0 package in R [28] was used to estimate the parameters of VBGMs. Graphs and statistical analyses were created and conducted in R [29].

## 3. Results

### *3.1. Length Size Structure*

Table S1 provides a comprehensive overview of the samples obtained throughout the various surveys conducted during the MEESO project, detailing characteristics such as the year, month, and area. Figure S1 shows the seasonal distribution of SL by region. A total of 2280 individuals were examined, comprising 2004 specimens from the Bay of Biscay (BoB), 442 from the Celtic Sea (CS), and 276 from the North Sea (NS). Additionally, to enhance the size range and sample size in the CS, data from samples collected by SINTEF in May 2017 (147 individuals) and July 2016 (50 individuals) were incorporated into the database [21].

The SL of the individuals ranged between 18 and 52 mm, 15 and 52 mm, and 25 and 59 mm in the BoB, CS, and NS, respectively. The total weight and standard length (both variables log-transformed) showed a strong positive linear relationship, indicating an exponential relationship between the untransformed variables (adjusted $r^2 > 0.96$, $p < 0.001$, Table 3). The ANCOVA analysis for TW-SL relationships between regions indicated that the null hypothesis of equality of the regressions was rejected ($p < 0.05$).

**Table 3.** Parameters and coefficients of the total weight (TW) vs. SL models for each region. $TW_{40mm}$ and $TW_{60mm}$ refer to the estimated weight for an individual of 40 mm and 60 mm SL, respectively.

| Area | b | SE_b | a | SE_a | $R^2$ adj | *p* | $TW_{40mm}$ | $TW_{60mm}$ |
|---|---|---|---|---|---|---|---|---|
| ALL | 3.03 | $1.02 \times 10^{-2}$ | $9.92 \times 10^{-6}$ | $3.67 \times 10^{-2}$ | 0.96 | <0.001 | 0.71 | 2.42 |
| NS | 3.17 | $3.99 \times 10^{-2}$ | $5.71 \times 10^{-6}$ | $1.46 \times 10^{-1}$ | 0.96 | <0.001 | 0.68 | 2.48 |
| CS | 2.93 | $2.36 \times 10^{-2}$ | $1.39 \times 10^{-5}$ | $8.77 \times 10^{-2}$ | 0.96 | <0.001 | 0.69 | 2.25 |
| BoB | 3.11 | $1.13 \times 10^{-2}$ | $7.85 \times 10^{-6}$ | $4.00 \times 10^{-2}$ | 0.97 | <0.001 | 0.76 | 2.70 |

The slopes varied from 2.93 to 3.17 (Table 3), and the *t*-test showed that the null hypothesis of equality of the regression coefficient H0: b =3 was exclusively rejected for the BoB (*t*-test = 2.84, df = 1997, $p < 0.05$). According to the models (Figure 3), for a similar SL, the difference in weight for *M. muelleri* between regions was barely noticeable for sizes less than 30 mm SL; however, for larger individuals, the difference progressively increased for the BoB population.

A pairwise analysis of covariance (ANCOVA) was applied to the three regions, which yielded statistically significant differences between the parameters of the weight-to-length models for all regions. In particular, the intercepts and slopes were statistically significant for all the pairs of regions ($F > 48.7$, $p < 0.001$), except for the slope for the pair BoB and NS ($F = 2.78$, $p = 0.06$).

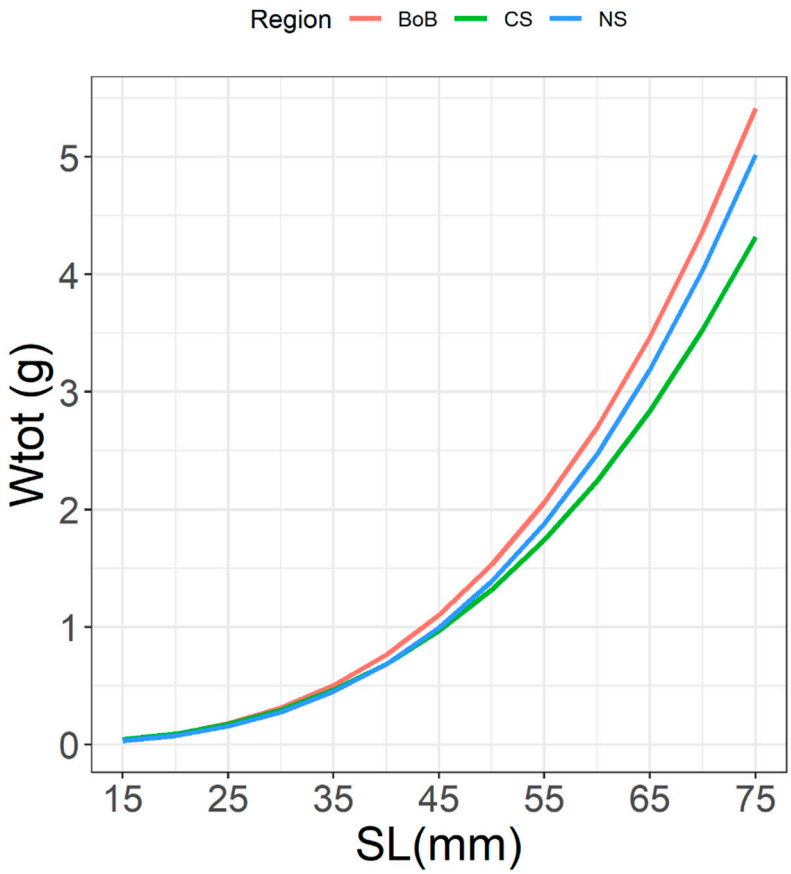


**Figure 3.** Curves of potential models of the total weight (Wtot) with length (SL) by area. Equations are those shown in Table 3.

### *3.2. Stomach Somatic Index (SSI)*

The SSI ranged from 0.56% to 13%, and means differed statistically between regions (Table 4, Kruskal–Wallis, $X^2 = 188.77$, $p < 0.001$). The relative stomach weight was significantly greater in the BoB than in the other two regions, with the lowest values recorded in individuals captured in the NS. Variability in the index was notably higher in the CS, whereas relative stomach weights showed greater homogeneity in the NS.

**Table 4.** Mean, standard deviation (±sd) and median values of SSI (in %) by regions. N = number of individuals.

| Region | Mean | Median | N |
|---|---|---|---|
| BoB | 5.86 ± 3.51 | 5.08 | 1365 |
| CS | 5.36 ± 5.36 | 3.87 | 226 |
| NS | 3.24 ± 1.86 | 3.05 | 263 |

### *3.3. Otolith Analysis*

Our data revealed that differences in longevity and growth occurred between regions. No specimens older than 4 years were found, except for one in the NS region. Furthermore, specimens older than 2 years were not found in either the CS or the BB (see Section 3.4. Age group 0 was the most abundant in the BoB and NS regions, whereas in the CS, it was age group 2. For age group 0, the mean SL ranged from 22.3 mm to 31.5 mm; for age group 1, the mean SL ranged from 38.9 mm to 48.6 mm; and finally, for age 2, the mean SL ranged from 44.2 mm to 52.3 mm (Table 5). Comparisons were conducted for all data pooled (all regions) and by region. First, the Kruskal–Wallis test for pooled data confirmed that the mean SL differed statistically between age groups ($p < 0.001$). Secondly, when data

were divided into age groups and regions, regional differences were also observed (Table 6, Kruskal–Wallis test $p < 0.001$). The Dunn test showed (Table 6) that, except for age groups 0 and 1 and the BB and NS regions, for the rest of the comparisons, there were statistically significant differences (adjusted $p$-value < 0.001).

**Table 5.** Mean SL and standard deviation (SD) of fish by age group and by region.

| | BoB | | CS | | NS | |
|---|---|---|---|---|---|---|
| **Age** | **SL** | **SD** | **SL** | **SD** | **SL** | **SD** |
| 0 | 27.47 | 4.4 | 22.26 | 3.02 | 31.53 | 2.81 |
| 1 | 41.92 | 4.95 | 38.87 | 6.81 | 48.6 | 4.95 |
| 2 | 44.21 | 3.31 | 45.77 | 4.99 | 52.27 | 5.1 |
| 3 | na | | na | | 53.94 | 3.87 |
| 4 | na | | na | | 63 | na |

**Table 6.** Dunn's test coefficients (Z) for multiple comparisons of the mean SL by age group and by region.

| **Dunn Test** | **Age 0** | | **Age 1** | | **Age 2** | |
|---|---|---|---|---|---|---|
| **Regions** | **Z** | **P-adj** | **Z** | **P-adj** | **Z** | **P-adj** |
| BoB-CS | 7.185 | <0.001 | 7.337 | <0.001 | −8.838 | <0.001 |
| BoB-NS | −1.543 | 0.368 | 2.582 | 0.0294 | −4.969 | <0.001 |
| CS-BoB | −7.75 | <0.001 | −5.899 | <0.001 | 5.673 | <0.001 |

The otolith radius (OR) ranged between 446 and 1052 µm (Figure 4). The relationship between OR and SL was described by a linear function (Figure 4). The F-test for OR and SL between regions showed that the null hypothesis of equality between the regressions was accepted, so common regression for all regions was estimated.

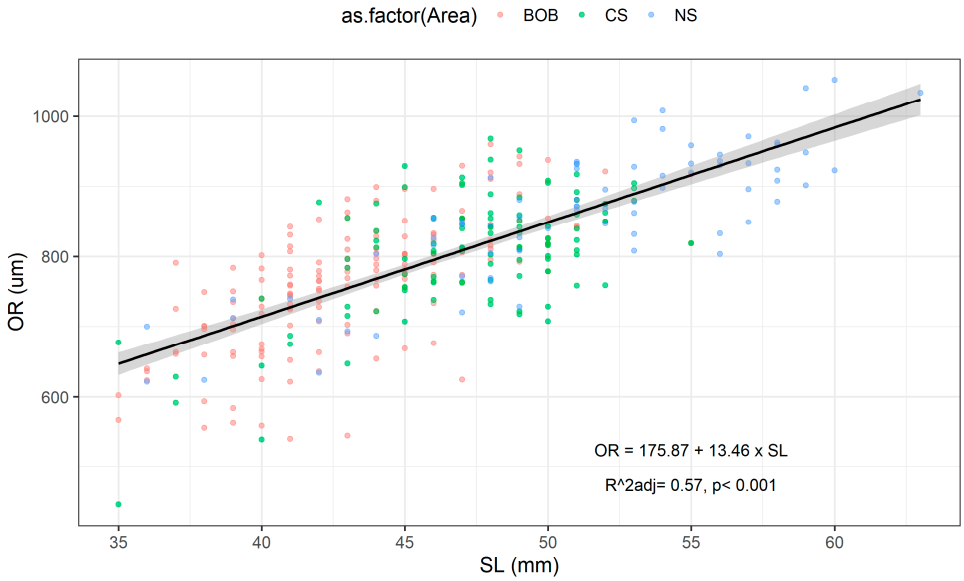


**Figure 4.** The otolith diameter (OR) and standard length relationship by regions of *M. muelleri* in the BoB (red dots), CS (green dots), and NS (blue dots). The common linear regression is shown in the panel.

The relationship between the radio of the otolith at the start of the translucent zone (winter zone, OR) and the SL of fish by age is shown in Figure 5. In the three regions, there was a significant relationship between both variables ($p$-values $\leq 0.05$); however, for age

group 1, the SL explained about 67% of OR variability, while for age group 2, the SL only explained 22% of its variability.

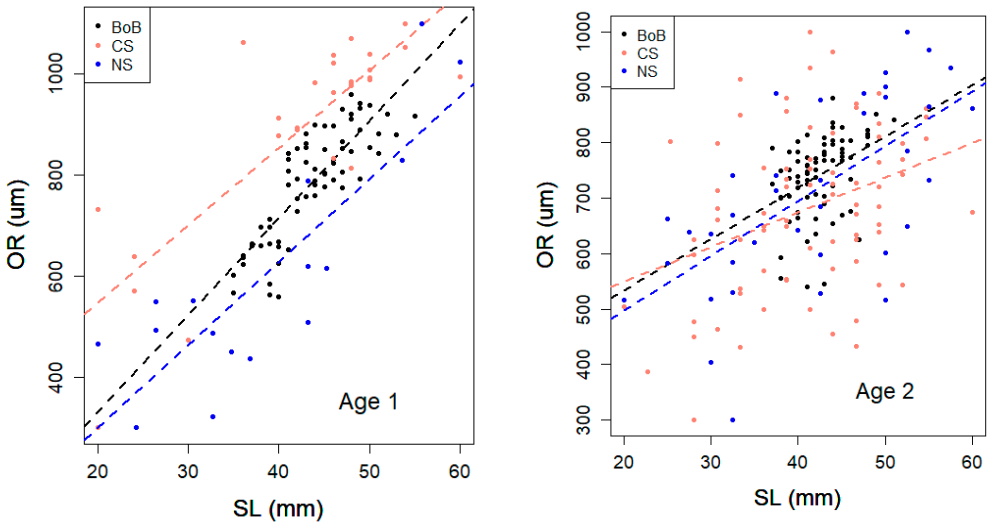


**Figure 5.** The radio at the start of the translucent (winter) zone in the otolith and the standard length of fish for age groups 1 and 2. The three regions are identified by different colours.

Figure 6 illustrates the pattern of increment formation, revealing that each annulus displays a single-peaked distribution. There is a consistent decrease in increment width as age progresses from 1 to 3. This decrease in increment widths aligns with the expected trend of a declining growth rate in the otolith with advancing age.

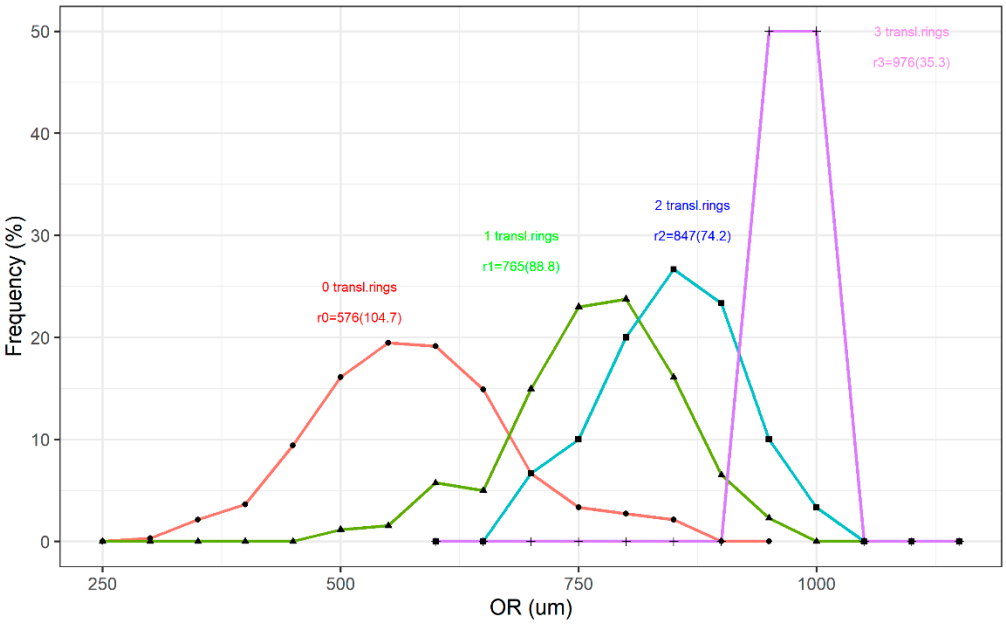


**Figure 6.** The pattern of the increment formation for otoliths with 0–3 translucent rings. R is the mean size (SD) of the radio. Data from the three regions were combined.

To evaluate whether the Lee phenomenon was observed in these populations, the mean residuals of the regression equation between the otolith radius and the standard length were calculated for the three areas (Table 7). The mean residual for the OR in the NS individual was higher than for the remaining areas; however, the analysis revealed that it did not differ statistically ($F = 2.01$, $p = 0.136$) between areas.

**Table 7.** The mean residual values from the SL vs. OR linear regression relationship by study region. SE = standard error.

| Region | Mean Residual | SE | N |
|---|---|---|---|
| BoB | −1.69 | 7.599 | 143 |
| CS | 0.78 | 6.304 | 110 |
| NS | 2.13 | 6.201 | 75 |

Regarding daily growth, the otoliths of a subsample of 11 individuals ranging in size between 21 and 33 mm were analysed. The estimated ages (in days) ranged from 104 to 157 days (Figure 7a), indicating that their birth date varied between 30 March and 24 May.

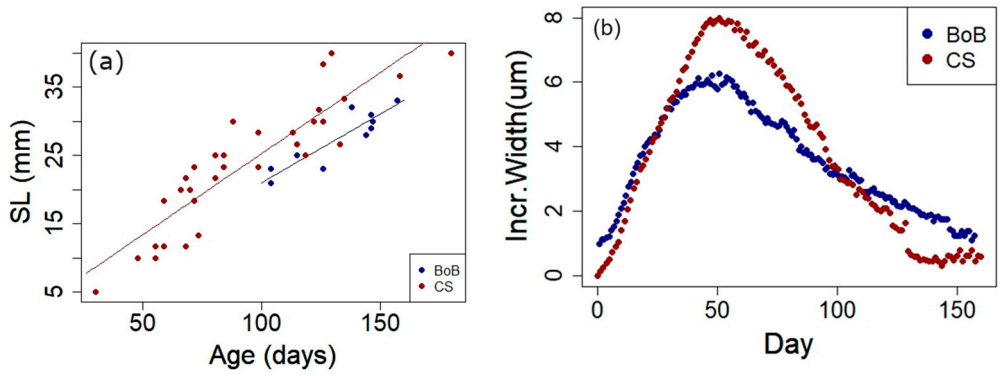


**Figure 7.** (**a**) SL (mm)–age (days) relationships for age 0 *M. muelleri* in the BoB (black points) and in the CS (red points, ref. [21]). Linear model equations for the BoB and the CS are as follows: SL = 0.896 + 0.201 × age and SL = 4.88 + 0.26 × age, respectively. (**b**) Daily increment width–day relationships for age 0 *M. muelleri* in the BoB (black points) and in the CS (red points, ref. [21]).

An analysis of the otolith microstructures revealed the presence of micro-increments, assumed to be deposited daily, in the otoliths of *M. muelleri*. These micro-increments exhibited a bipartite structure composed of an opaque zone and a hyaline zone deposited in concentric layers around a nucleus. The radius of this nucleus was 8.41 ± 0.96 µm (mean ± S.D.). Sub-daily micro-increments were observed and were easily distinguished by the following [30].

The relationship between the number of micro-increments (age) and the standard size was high and significant, described by a linear relationship (Figure 7a) in the following equation:

$$SL = 0.896 + 0.201 \times Age \ (r^2 = 0.817, df = 10).$$

Accordingly, the estimated growth rate for *M. muelleri* individuals in the Bay of Biscay was 0.20 mm day$^{-1}$.

The daily growth pattern of the otolith showed a progressive increase in the widths of micro-increments, reaching their widest between days 42 and 51, with a maximum average width of 6.01 ± 1.22 µm. Subsequently, the widths decreased significantly until the time of capture (Figure 7b).

For comparison purposes, we included the daily growth equation reported by this species in the CS region in 2016 ([21], Figure 7a,b). As the figures illustrate, the daily growth of *M. muelleri* was 30% higher than that observed in the BoB (Figure 7a), with the maximum increment width occurring between days 38 and 41, slightly preceding that of the BoB.

### *3.4. Von Bertalanffy Growth Models (VBGM)*

The von Bertalanffy parameters by region are shown in Table 8 and the curves in Figure 8.

**Table 8.** Parameters and coefficient of variation (CV) of each estimated parameter of VBG models by region. N = number of individuals.

| Region | $SL_{inf}$ (mm) | CV | K | CV | to | CV | N |
|---|---|---|---|---|---|---|---|
| BoB | 45.14 | 0.007 | 1.84 | 0.092 | −0.025 | 1.745 | 1574 |
| CS | 50.3 | 0.018 | 1.25 | 0.14 | −0.075 | 0.981 | 335 |
| NS | 54.7 | 0.019 | 1.36 | 0.178 | −0.145 | 0.063 | 262 |

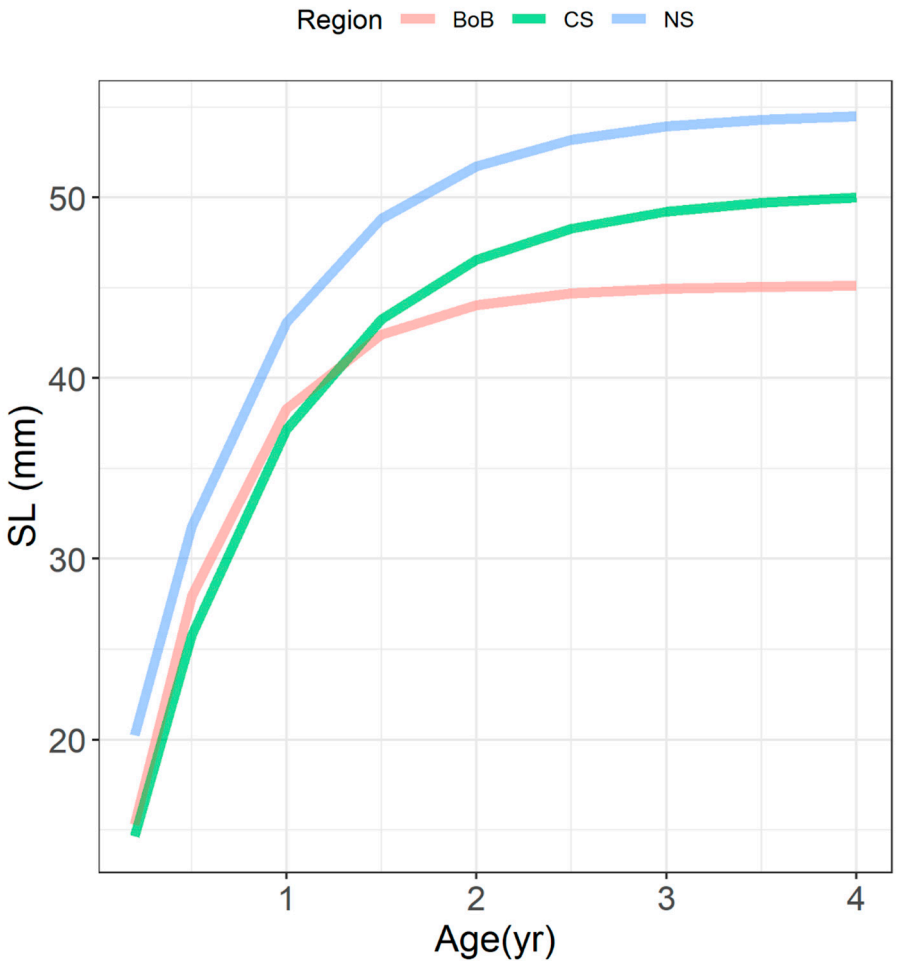


**Figure 8.** The curve of VB growth models by region: BoB in red, CS in green, and NS in blue. The values are those in Table 8.

The relationships between the number of annual increments and SLs resulted in an asymptotic size ranging between 45.1 and 54.7mm that increased latitudinally from south to north. The estimate of $L_{inf}$ in the BoB (45.1 mm) was the lowest, while the highest was in the NS (54.7 mm, Table 8). For all regions, the CVs of the $L_{inf}$ coefficients were low.

The growth rate coefficients (*K*s) varied from 1.25 to 1.84 $year^{-1}$, with the highest estimate in the BoB (1.84 $year^{-1}$), intermediate in the NS (1.36 $year^{-1}$), and the lowest estimate in the CS (1.25 $year^{-1}$). The CV was notably high in the NS (0.178 $year^{-1}$) compared to the CI from the other regions. For NS and CS regions, the fixed fraction of the annual growth increments (calculated as $e^{-K}$ ([31]) showed an annual increase of 0.28 and 0.26, respectively. The estimates in the BoB (0.15) indicate that the annual growth increments were almost half of those estimated in the other regions.

The estimates of $t_o$ ranged between −0.025 and −0.14, with the highest estimates and CV (1.745) in the BoB. Similar estimates of this parameter in the BoB and CS suggest a closer spawning time in those regions.

## 4. Discussion

The findings of this study provide valuable insights into the growth dynamics and life history traits of *Maurolicus muelleri* across three regions of the Northeast Atlantic: the Bay of Biscay (BoB), the Celtic Sea (CS), and the North Sea (NS). By analysing length–weight relationships, otolith morphometry, and growth increments, we identified significant regional variations in the growth patterns, longevity, and otolith characteristics of *M. muelleri* populations.

In the context of global population dynamics, a recurring pattern was observed where larger individuals predominated in winter, while smaller individuals were more abundant in summer and autumn (Figure S1). During spring, the population appeared to be a mixture of individuals from different cohorts. Similar variations in length structure associated with seasons have been documented in the North Atlantic [6,21]. The latter observed juvenile *M. muelleri* during autumn and winter. At the same time, ref. [21] reported substantial variability in size structures from Portugal to Norway, with smaller fish dominating in May and larger fish in July.

The observed size increase with latitude aligns with Bergmann's rule, which posits that the body size tends to increase with decreasing temperature and increasing latitude. In our study, where the average temperatures tolerated by populations could differ by up to 10 degrees, this phenomenon was evident. While [32] suggested that Bergmann's rule in fish is tied to the species' thermal niche and applies primarily to coldwater species, our findings support its applicability to *M. muelleri*, a temperate and widely distributed species. This alignment with Bergmann's rule underscores the significance of temperature as one of the principal factors influencing the body size of this mesopelagic species.

The weight-to-length models are statistically different regionally and show how the difference in weight between individuals of different origins increases with length. These differences were also size-dependent, being practically imperceptible for small size ranges (<30 mm) and very evident for larger size ranges (>45 mm). In general, in the BoB, individuals were the heaviest (8% and 19% heavier than a similar fish in the CS and NS, respectively) and in the NS, they were the lightest. All these variations are usually related to light, temperature, and food availability [5,33]. *M. muelleri* is a visual predator and is characterised by diel vertical migration. Light intensity and the photoperiod are factors with considerable variability in latitude and season and may affect its feeding opportunities. As direct measurements of food availability were not available, we used the Stomach Somatic Index (SSI) as a proxy for the feeding status of the fish at the time of capture (Table 4). This index was statistically higher in the BoB and was minimal in the NS. This finding appears to support the aforementioned observations. Certainly, this index only reflects a specific condition and can indeed be influenced by the time of day at which individuals were captured and the season. It is well documented that this species undergoes nocturnal vertical migrations to the surface for feeding [2,34,35]. In our study, all samples were taken during the day, which is not thought to correspond to periods of peak feeding activity. The temperature within the optimal range for the species promotes the growth of individuals under similar food conditions. In natural settings, food availability is typically not critical, so given the limited data available and the constraints they impose on further analysis, it is reasonable to infer that the better condition of *M. muelleri* in the BoB can be attributed to a more conducive growth environment for this population, particularly in terms of temperature and light intensity.

Knowing how the otolith grows with body size is essential for the correct use of otoliths as a tool for age determination. We found that the relationship between otolith diameter and standard length was linear, with no significant differences among regions. In the absence of validation of the annual growth ring formation in *M. muelleri*, we demonstrated that the deposition of annual rings follows the ring position across the otolith (Figure 6). Moreover, the relationship of the otolith radius with size loses robustness when individuals of ages 1 and 2 are analysed separately (Figure 5). This is interpreted to mean that the

variability in OR is primarily due to differences in the growth rate rather than differences in birth date as the fish grow.

Many studies have shown that the otoliths of slow-growing fish tend to be larger and heavier than those of fast-growing fish of the same size, whether on a daily or annual basis (Lee's phenomenon, ref. [11]). This means care should be taken when back-calculating the lengths of a species where a growth rate effect on otolith size is known or suspected to occur. In particular, ref. [11] observed that this phenomenon occurs to some extent in most populations of *M. muelleri* from fjords or the Norwegian Sea.

Lee's phenomenon was investigated to determine whether the unexplained variability in the otolith radius, as observed in the model, could be attributed to differences in otolith size resulting from variations in growth rates among populations (Table 5). The analysis of residuals by regions revealed that otoliths were slightly smaller in the BoB (mean residuals = −1.69) and larger in the NS (mean residuals = 2.13). However, as the differences between areas were not significant, we cannot conclude that this phenomenon actually occurred. If the phenomenon exists, as [4] reported and [11] suggested, pooling data for different periods and year classes (Figure 9) might likely hide it as we gathered individuals with diverse growth rates in the same area.

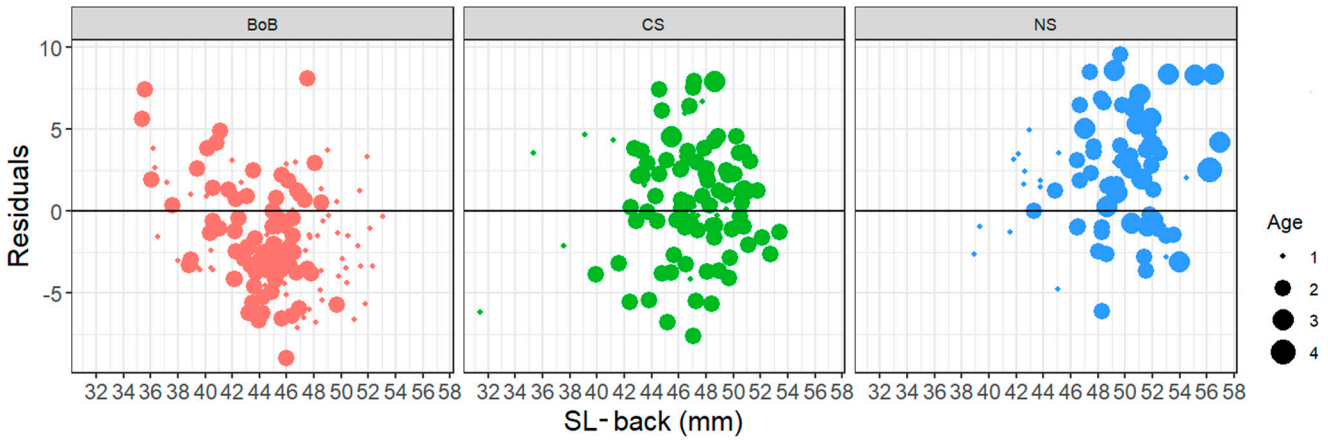


**Figure 9.** Otolith radius residuals and the back-calculated SL for regions. The size of the dots is proportional to the age of the fish.

Therefore, the back-calculated length from the annual increment in the otolith seems to be a reliable proxy for estimating fish size throughout the entire lifespan of the fish regardless of the area in which they grew. This characteristic is essential if otoliths are to be used as a tool for age determination.

*M. muelleri* is a short-lived species with variable longevity associated with its geographic origin. We also observed a large variability in the size range between individuals in similar age groups. This was especially notable in the age 0 group of the BoB, and this trait is associated with species with a long spawning season, which would generate a wide size range of age 0 individuals. In this line, the range of 30–40 mm for age-0-group fish observed in the area of Rockall Trough [6] supported our results. Regionally, we saw that the means of SL for age 0 and age 1 were not significantly different for the BoB and NS, probably due to the high variability observed. This is in contrast to what is reported in the literature, where a variation in mean SL for age groups 0 and 1 linked to different geographical locations was noted in Norwegian waters [4].

The estimated mean somatic growth rate for *M. muelleri* in the BoB (0.20 mm day$^{-1}$) is comparable to that reported by [36], who studied the growth of *M. muelleri* larvae in a Norwegian fjord (0.20 mm day$^{-1}$), and slightly lower than the estimate for juveniles in the CS area (0.26 mm day$^{-1}$) [21]. Slower growth rates were also observed in other congeners: *M. stehmanni* in Brazilian waters (0.19 mm day$^{-1}$) [37], *M. australis* larvae (0.16 mm day$^{-1}$) in Chilean Patagonia [38], and *M. mucronatus* (0.15 mm day$^{-1}$) in the Red

Sea [39]. Excluding the growth rate reported for this species in the CS, this parameter slightly varied from 0.15 to 0.20 mm day$^{-1}$ in habitats as diverse as the Red Sea or Brazilian waters. The highest somatic growth rate detected during the juvenile stages in the CS aligns well with the increased length-at-age observed in this population during adulthood (Figure 7).

The $L_{inf}$ estimated for *M. muelleri* varied from 45.1 mm to 54.7 mm. In different regions, seasons, and sexes, previous studies reported $L_{inf}$ in accordance with our estimates (values ranged from 43.8 to 59.4 mm; see Figure 9). Our results show that Linf is positively correlated with latitude. In general, ectotherms grow slower and achieve a larger size at higher latitudes (Bergamnn's rule). The maximum age found in this study also differed latitudinally; in fish collected in the NS, it was 4 years (which is close to the maximum age reported in the literature (5 years, ref. [36]), while in the other regions studied, no fish older than 2 years were collected. These findings are in good agreement with the information compiled from the literature. In fjords and offshore waters, only a few individuals reach the age of 3 or 3.5 years [4]. In the Rockall Trough, no fish older than 2 years were found [6]. The authors attributed the absence of fish older than this age to the high mortality that big spawners would experience after spawning.

The estimates of the growth rate (K) match those reported in the literature (1.25–1.86). The highest value was estimated in the area of the BoB, and the lowest was in the CS. If K measures the exponential rate of approach to the asymptotic size [31], *M. muelleri* from CS and NS regions showed similar growing rates (0.286 and 0.26, respectively), which leads to the interpretation that the larger sizes observed in the NS could be ascribable to greater longevity in this region.

The effect of environmental conditions on fish growth has been widely reported [5,12]. Temperature, food availability, food quality, and light can significantly impact their growth and cause the spatial variability observed. Due to data limitations, we constructed growth curves by combining samples from different seasons and years. Consequently, the seasonal variability within a region could be the same magnitude as the variability between two regions. Comparing samples from the Norwegian Sea, coast, and fjords, significant differences in life history parameters attributed to different environmental and ecological factors were denoted [12]. In this context, the growth curves should be considered as a general growth model that represents the average growth under a wide range of environmental conditions.

A balance between the growth rate (K) and the maximum size ($L_{inf}$) is frequently found. This balance is influenced by several factors. Temperature is well known to play a crucial role in the growth and metabolism of marine fish. In general, higher temperature regimes accelerate growth. In addition to temperature, food availability is another major factor affecting growth. It has been shown that increasing food availability causes a shift toward a larger maximum length [40–42] but may not increase the growth rate. In fjordic and oceanic environments, the authors of [5] noted that differences in the resource levels may offset the negative relationship between the growth rate and the maximum length [40,43,44]. In Figure 10, the parameters K and $L_{inf}$ of the VBG model obtained from different sources are represented. Most of the information refers to fjord habitats (non-numbered dots), and a few pieces of information refer to open waters (numbered dots). We included the data obtained in this study to examine how they compare with those from the literature. The absence of a correlation between the parameters of the VBG model reinforces the aforementioned assertion regarding the effect of environmental conditions on the trade-off between K and $L_{inf}$. Moreover, if the relationship of VBG parameters depends on the environmental conditions in which fish live, the values of BoB and CS seem to reflect conditions similar to those found in fjords, while those of NS resemble those of open sea. These results also underscore the complexity of comparing populations living in different environmental regimes.

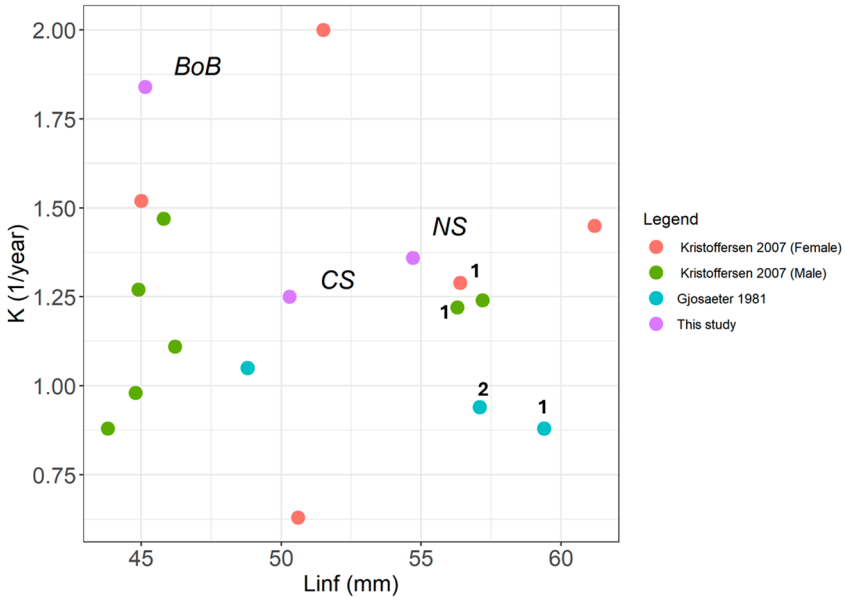


**Figure 10.** VBGM parameters. The relationship between K (1/year) and $L_{inf}$ (mm) for *M. muelleri*. Legend: Orange and green colours refer to female and male parameters data from [10]; blue and violet colours refer to data from [4]; and this study's data include males and females combined. These study areas are marked in the panel as BoB, CS, and NS. Most of the information comes from fjord habitats, and those from open waters and fjords–open waters combined are marked with (1) and (2), respectively.

## 5. Conclusions

This study investigated the growth patterns of *M. muelleri* in the Northeast Atlantic from an extensive geographical perspective and provided information on the regional variability in common key biological parameters, such as length–weight relationships and VBG parameters. Length–weight relationships revealed better conditions for individuals inhabiting the Bay of Biscay (BoB), which was associated with a better feeding status. Otolith growth was described well by linear regression, and growth was not statistically different between regions. Lee's phenomenon was not observed, likely due to the mixing of individuals with diverse growth rates. Annual ring formation was confirmed by plotting the distance from the otolith core to the ring position for each age group. Longevity and Linf increased progressively northwards in accordance with Bergmann's rule. In terms of annual growth, the highest growth was estimated for the BoB, and the lowest was in the Celtic Sea (CS). This regional pattern may be related to the superior fish conditions observed in that region. Concerning daily growth, the trend between the BoB and the CS was the opposite; in the latter, growth during the first year of life was 30% higher than that in the BoB. The observed biological variability has been attributed to differences in the environment in which the organisms in question live. Nevertheless, it remains unclear whether these populations constitute discrete population units. Without more information, our results provide new evidence of the biological diversity of this population.

**Supplementary Materials:** The following supporting information can be downloaded at: https://www.mdpi.com/article/10.3390/fishes9070250/s1, Figure S1: Quarterly variability of SL (mm) of *M. muelleri* by regions; Table S1: Summary of main characteristics of samples collected in the Bay of Biscay, Celtic Sea, and in the Norwegian Sea, respectively by year, month and sex.

**Author Contributions:** P.A.: conceptualisation, formal analysis, writing—original draft. N.A.: validation, writing—review and editing. A.M.W., T.C., and G.B.: investigation and writing—review and editing. E.G., W.M., and T.K.: investigation. All authors have read and agreed to the published version of the manuscript.

**Funding:** This study was supported by the European Union's Horizonte 2020 program (MEESO project, H2020-LC-BC-03-2018) and the Dpto. Desarrollo Económico, Sostenibilidad y Medio Ambiente. Vice. de Agricultura, Pesca y Política Alimentaria, Dirección de Pesca y Acuicultura of the Basque Government (MESOPEL and MECOSIS projects). This paper is a contribution Nº 1227 from AZTI, Marine Research, Basque Research and Technology Alliance (BRTA).

**Institutional Review Board Statement:** Ethical review and approval of this study has been waived because there has been no animal testing. The animals were caught with fishing nets and arrive on the ship already dead. So, the study did not require ethical approval.

**Informed Consent Statement:** Not applicable.

**Data Availability Statement:** Data are available upon request to the corresponding author.

**Conflicts of Interest:** The authors declare no conflicts of interest. The funders (European Union's Horizon 2020 research and innovation program) had no role in the design of the study; in the collection, analyses, or interpretation of data; in the writing of the manuscript; or in the decision to publish the results.

## References

1. Rees, D.J.; Poulsen, J.Y.; Sutton, T.T.; Costa, P.A.S.; Landaeta, M.F. Global phylogeography suggests extensive eucosmopolitanism in Mesopelagic Fishes (Maurolicus: Sternoptychidae). *Sci. Rep.* **2020**, *10*, 20544. [CrossRef]
2. Sobradillo, B.; Boyra, G.; Martinez, U.; Carrera, P.; Peña, M.; Irigoien, X. Target strength and swimbladder morphology of Mueller's pearlside (*Maurolicus muelleri*). *Sci. Rep.* **2019**, *9*, 17311. [CrossRef] [PubMed]
3. Caiger, P.E.; Lefebve, L.S.; Llopiz, K. Growth and reproduction in mesopelagic fishes: A literature review. *ICES J. Mar. Sci.* **2021**, *78*, 765–781. [CrossRef]
4. Gjøsæter, J. Life history and ecology of *Maurolicus muelleri* (Gonostimatidae) in Norwegian waters. *Fisk. Skr. Ser. Havunders.* **1981**, *17*, 109–131.
5. Kristoffersen, J.B.; Salvanes, A.G.V. Life history of *Maurolicus muelleri* in fjordic and oceanic environments. *J. Fish Biol.* **1998**, *53*, 1324–1341. [CrossRef]
6. Kawaguchi, K.; Mauchline, J. Biology of Sternoptychid Fishes Rockall Trough; Northeastern Atlantic Ocean. *Biol. Oceanogr.* **1987**, *4*, 99–120.
7. Carbonara, P.; Follesa, M.C. (Eds.) *Handbook on Fish Age Determination: A Mediterranean Experience*; Studies and Reviews 2019, No. 98; FAO: Rome, Italy, 2019; 192p.
8. Casas, M.C. Increment formation in otoliths of slow-growing winter flounder (Pleuronectes americanus) larvae in cold water. *Can. J. Fish. Aquat. Sci.* **1998**, *55*, 162–169. [CrossRef]
9. Cassoff, R.M.; Campana, S.E.; Myklevoll, S. Changes in baseline growth and maturation parameters of Northwest Atlantic porbeagle; Lamna nasus; following heavy exploitation. *Can. J. Fish. Aquat. Sci.* **2007**, *64*, 19–29. [CrossRef]
10. Kristoffersen, J.B. Growth rate and relative otolith size in populations of adult Muller's pearlside *Maurolicus muelleri*. *J. Fish Biol.* **2007**, *71*, 1317–1330. [CrossRef]
11. Lee, R.M. An investigation into the methods of growth determination in fishes. *Cons. Perm. Int. Explor. Mer Hbl. Circonstance* **1912**, *63*, 35.
12. Salvanes, A.G.V.; Stockley, B.M. Spatial variation of growth and gonadal developments of *Maurolicus muelleri* in the Norwegian Sea and in a Norwegian fjord. *Mar. Biol.* **1996**, *126*, 321–332. [CrossRef]
13. ICES. Working group on Mackerel and horse mackerel eggs surveys (WGMEGS). *ICES Sci. Rep.* **2023**, *5*, 118. [CrossRef]
14. Racault, M.-F.; Le Quéréc, C.; Buitenhuis, E.; Sathyendranath, S.; Platt, T. Phytoplankton phenology in the global ocean. *Ecol. Indic.* **2012**, *14*, 152–163. [CrossRef]
15. Ellingsen, I.H.; Dalpadado, P.; Slagstad, D.; Loeng, H. Impact of climatic change on the biological production in the Barents Sea. *Clim. Chang.* **2008**, *87*, 155–175. [CrossRef]
16. Boyra, G.; Martinez, U.; Cotano, U.; Santos, M.; Irigoien, X.; Uriarte, A. Acoustic surveys for juvenile anchovy in the Bay of Biscay: Abundance estimate as an indicator of the next year's recruitment and spatial distribution patterns. *ICES J. Mar. Sci.* **2013**, *70*, 1354–1368. [CrossRef]
17. Alvarez, P.; Korta, M.; Garcia, D.; Boyra, G. Life-History Strategy of *Maurolicus muelleri* (Gmenlin; 1789) in the Bay of Biscay. *Hydrobiology* **2023**, *2*, 289–313. [CrossRef]
18. O'Donnell, C.; O´Malley, M.; Smith, T.; O´Brien, S.; Mullins, E.; Connaughton, P.; Tadeo, M.P.; Barile, C. *Western European Shelf Pelagic Acoustic Survey (WESPAS). 3 June–12 July 2020. FEAS Survey Series: 2020/03*; Marine Institute: Galway, Ireland, 2020; Available online: http://hdl.handle.net/10793/1659 (accessed on 17 June 2024).
19. O'Donnell, C.; O'Malley, M.; Mullins, E.; Connaughton, P.; Keogh, N.; Croot, P. *Western European Shelf Pelagic Acoustic Survey (WESPAS), 9 June–20 July 2021. FEAS Survey Series: 2021/03*; Marine Institute: Galway, Ireland, 2021; Available online: http://hdl.handle.net/10793/1720 (accessed on 17 June 2024).

20. ICES. Report on the Working Group on International Blue whiting spawning stock survey (IBWSS) spring 2021. In *WD on Widely Distributed Stocks*; International Council for the Exploration of the Sea (ICES): Copenhagen, Denmark, 2021.
21. Grimaldo, E.; Grimsmo, L.; Alvarez, P.; Herrmann, B.; Møen Tveit, G.; Tiller, R.; Slizyte, R.; Aldanondo, N.; Guldberg, T.; Toldnes, B.; et al. Investigating the potential for a commercial fishery in the Northeast Atlantic utilizing mesopelagic species. *ICES J. Mar. Sci.* **2020**, *77*, 2541–2556. [CrossRef]
22. Ottersen, G. A digital temperature atlas for the Norwegian Sea. *ICES J. Mar. Sci.* **2010**, *67*, 1525–1537. [CrossRef]
23. ICES. *Report of the Workshop on Age Reading of European Anchovy (WKARA) 2010, 9–13 November 2009*; ICES CM 2009/ACOM:43 2010; ICES: Sicily, Italy; pp. 9–13. [CrossRef]
24. Aldanondo, N.; Cotano, U.; Tiepolo, M.; Boyra, G.; Irigoien, X. Growth and movement patterns of early juvenile European anchovy (*Engraulis encrasicolus* L.) in the Bay of Biscay based on otolith microstructure and chemistry. *Fish. Oceanogr.* **2010**, *19*, 196–208. [CrossRef]
25. Sokal, R.R.; Rohlf, F.J. *Biometry: The Principles and Practice of Statistics in Biological Research*, 4th ed.; W.H. Freeman and Company: New York, NY, USA, 2012.
26. Sachs, L. *Applied Statistics: A Handbook of Techniques*; Springer: Berlin/Heidelberg, Germany, 1982; 706p.
27. Le Cren, E.D. The length-weight relationship and seasonal cycle in gonad weight and condition in the perch (*Perca fluviatilis*). *J. Anim. Ecol.* **1951**, *20*, 201–219. [CrossRef]
28. Sampedro, P.; Saínza, M.; Trujillo, V. Inbio 2.0 Manual. A simple tool to calculate biological parameter's uncertainty. 2013. [CrossRef]
29. R Core Team. R: A Language and Environment for Statistical Computing. R Foundation for Statistical Computing. 2021. Available online: https://www.R-project.org/ (accessed on 15 January 2024).
30. Campana, S.E. Measurement and interpretation of the microstructure of fish otoliths. *Can. Spec. Publ. Fish. Aquat. Sci.* **1992**, *117*, 59–71.
31. Schnute, J.T.; Fournier, D.A. A new approach to length-frequency analysis: Growth structure. *Can. J. Fish. Aquat. Sci.* **1980**, *37*, 1337–1351. [CrossRef]
32. Rypel, A.L. The cold-water connection: Bergmann's in North American freshwater fishes. *Am. Nat.* **2014**, *183*, 147–156. [CrossRef] [PubMed]
33. Kaartvedt, S.; Knutsen, T.; Holstz, J.C. Schooling of the vertically migrating mesopelagic fish *Maurolicus muelleri* in light summer nights. *Mar. Ecol. Prog. Ser.* **1998**, *170*, s287–s290. [CrossRef]
34. deBusserolles, F.; Cortesi, F.; Helvik, J.V.; Davies, W.I.L.; Templin, R.M.; Sullivan, R.K.P.; Michell, C.T.; Mountford, J.K.; Collin, S.P.; Irigoien, X.; et al. Pushing the limits of photoreception in twilight conditions: The rod-like cone retina of the deep-sea pearlsides. *Sci. Adv.* **2017**, *3*, eaao4709. [CrossRef] [PubMed]
35. Christiansen, S.; Klevjer, T.A.; Røstad, A.; Aksnes, D.L.; Kaartvedt, S. Flexible behaviour in a mesopelagic fish (*Maurolicus muelleri*). *ICES J. Mar. Sci.* **2021**, *78*, 1623–1635. [CrossRef]
36. Folkvord, A.; Gundersen, G.; Albretsen, J.; Asplin, L.; Kaartvedt, S.; Giske, J. Impact of hatch date on early life growth and survival of Mueller's pearlside (*Maurolicus muelleri*) larvae and life-history consequences. *Can. J. Fish. Aquat. Sci.* **2016**, *73*, 163–176. [CrossRef]
37. Bellucco, A.; Hara, A.; Machado Almeida, E.; del Bianco Rossi-Wongtschowski, C.L. Growth parameters estimates of Maurolicus stehmanni Parin and Kobyliansky 1996 (Teleostei; Sternoptichydae) from south and southeastern Brazilian waters. *Braz. J. Oceanogr.* **2004**, *52*, 195–205. [CrossRef]
38. Landaeta, M.F.; Bustos, C.A.; Contreras, J.E.; Salas-Berríos, F.; Palacios-Fuentes, P.; Alvarado-Niño, M.; Balbontín, F. Larval fish feeding ecology; growth and mortality from two basins with contrasting environmental conditions of an inner sea of northern Patagonia; Chile. *Mar Environ. Res* **2015**, *106*, 19–29. [CrossRef] [PubMed]
39. Aldanondo, N.; Kaartvedt, S.; Irigoien, X. Growth patterns of two Read Sea mesopelagic fishes. *Mar. Biol.* **2023**, *170*, 8. [CrossRef]
40. Beverton, R.J.H.; Holt, S.J. On the dynamics of exploited fish populations. *Fish. Investig.* **1957**, *19*, 1–533.
41. Beverton, R.J. Longevity in fish: Some ecological and evolutionary considerations. *Basic Life Sci.* **1987**, *42*, 161–185. [PubMed]
42. Walters, C.J.; Post, J.R. Density-dependent growth and competitive asymmetries in size-structured fish populations: A theoretical model and recommendations for field experiments. *Trans. Am. Fish. Soc.* **1993**, *122*, 34–45. [CrossRef]
43. Froese, R.; Binohlan, C. Empirical relationships to estimate asymptotic length; length at first maturity and length at maximum yield per recruit in fishes; with a simple method to evaluate length frequency data. *J. Fish Biol.* **2000**, *56*, 758–773. [CrossRef]
44. Pilling, G.M.; Kirkwood, G.P.; Walker, S.G. An improved method for estimating individual growth variability in fish; and the correlation between von Bertalanffy growth parameters. *Can. J. Fish. Aquat. Sci.* **2002**, *59*, 424–432. [CrossRef]